Journal of Nuclear Materials 405 (2010) 17–27

Contents lists available at ScienceDirect

Journal of Nuclear Materials

journal homepage: www.elsevier.com/locate/jnucmat

Corrosion fatigue behavior of low alloy steels under simulated BWR coolant conditions

J.Y. Huang *, M.C. Young, S.L. Jeng, J.J. Yeh, J.S. Huang, R.C. Kuo

Institute of Nuclear Energy Research (INER), P.O. Box 3-14, 1000 Wenhua Road, Chiaan Village, Lungtan 325, Taiwan, ROC

ARTICLE INFO

Article history:
Received 11 August 2009
Accepted 21 July 2010

ABSTRACT

The corrosion fatigue crack growth behavior of A533 and A508 low alloy steels under simulated boiling water reactor (BWR) coolant conditions was studied. Corrosion fatigue crack growth rates of A533B3 and A508 cl. 3 steels were significantly affected by the steel sulfur content, loading frequency and dissolved oxygen content of water environments. The data points outside the bound of Eason's model could be attributed to the low frequency, higher steel sulfur content and high dissolved oxygen in water environments. The sulfur dissolved in the water environment from the higher-sulfur steels was sufficiently concentrated to acidify the crack tip chemistry even in the hydrogen water chemistry (HWC). Therefore, nitrogenated or HWC water showed little or no beneficiary effect on the high-sulfur steels. For the steel specimens of the same sulfur level, their corrosion fatigue crack growth rates were comparable in different orientations, which could be related to the exposure of fresh sulfides to the water environment. The percentages of sulfides per unit area, by quantitative metallography, were comparable for the steel specimens of both orientations. When the steel sulfur content was decreased to a critical sulfur content 0.005 wt.%, the crack growth rates decreased remarkably.

1. Introduction

Low carbon and low alloy steels, SA533 and SA508, are most commonly used for nuclear reactor pressure vessels (RPV) whose integrity governs the safety of nuclear power plants. Fatigue is one of the main degradation mechanisms affecting the pressure vessel integrity of pressurized water reactors (PWRs) and boiling water reactors (BWRs) [1–6]. The fatigue crack growth rates of RPV materials in simulated light water reactor (LWR) coolant environments are influenced by sulfur content, sulfide morphology [7–11] and orientation, water chemistry, loading frequency separately and synergistically [9,10,12–18]. The sulfur content has been reported to enhance the corrosion fatigue crack growth rates of low alloy steels [19]. However, little work has been done to study the threshold of sulfur content on the corrosion fatigue crack growth rates of RPV steels. Although the vessel steels of most of new nuclear reactors contain 0.008 wt.% sulfur or less, older vessels generally have higher levels of sulfur [20,21]. Hydrogen water chemistry (HWC) proves to be a powerful method for mitigating environmentally-assisted cracking (EAC) in stainless steel and nickel-base alloy components. Ritter and Seifert [22] demonstrated HWC resulted in a significant drop in low-frequency corrosion fatigue crack growth rates by at least one order of magnitude with respect to normal water chemistry (NWC) conditions for pressure vessel steels with sulfur content lower than 0.02 wt.%. It is of practical and academic interest to study the effect of HWC on the mitigation of corrosion fatigue cracking for low alloy steels with higher sulfur contents. The hypothesis that has been widely accepted to account for the crack propagation in the carbon and low alloy steels in LWR water systems is the slip-oxidation mechanism [23]. This mechanism relates crack advance to the oxidation rate that occurs at the crack tip. In order to better predict the crack growth rates of low alloy steels, the interaction between the oxide films and sulfur ion dissolved from steels in the oxygenated or HWC water environments should be clarified.

In this study, the corrosion fatigue crack growth tests were performed on A533B3 and A508 cl. 3 low alloy steels under simulated BWR coolant conditions. To investigate the sulfur content on the fatigue crack growth behavior of low alloy steels, A533B3 and A508 cl. 3 steel specimens with four and two sulfur content levels were prepared, respectively. Corrosion fatigue tests were conducted in different water chemistries including air saturated, deoxygenated by nitrogen and hydrogen. The fracture features of fatigued specimens were studied with optical stereography and scanning electron microscopy (SEM).

* Corresponding author. Tel.: +886 3 4711400; fax: +886 3 4711409.
E-mail address: jyhuang@iner.gov.tw (J.Y. Huang).

0022-3115/$ - see front matter © 2010 Elsevier B.V. All rights reserved.
doi:10.1016/j.jnucmat.2010.07.029

Table 1
Chemical compositions of A533B3 steels.

Designation	Composition (wt.%)									
	C	Si	Mn	P	S	Ni	Mo	A1	N	Fe
#1	0.207	0.22	1.28	<0.02	0.006	0.6	0.52	0.015	0.005	Bal.
Y1	0.19	0.22	1.22	0.015	0.008	0.60	0.49	0.035	0.005	Bal.
Y2	0.19	0.22	1.27	0.015	0.016	0.60	0.49	0.035	0.005	Bal.
Y3	0.21	0.23	1.25	0.015	0.027	0.60	0.49	0.035	0.005	Bal.

Solution treated at 900 °C for 1.5 h, then quenched and tempered at 670 °C for 1 h.

Table 2
Mechanical properties of A533B3 steels.

Designation	Temperature (°C)	Ultimate tensile strength (MPa)	Yield strength (MPa)	Total elongation (%)	Uniform elongation (%)
#1	25	722	650	29.5	10.2
	300	751	600	30.2	11.0
Y1	25	711	625	30.3	10.5
	300	692	510	31.1	13.2
Y2	25	686	600	30.6	10.3
	300	680	516	30.1	12.1
Y3	25	722	630	28.6	10.1
	300	722	550	31.2	13.2

Table 3
Chemical compositions of A508 cl. 3 steels.

Designation	Composition (wt.%)									
	C	Si	Mn	P	S	Ni	Mo	V	Cr	Fe
F1	0.16	0.21	1.35	0.005	0.005	0.76	0.57	0.014	0.13	Bal.
F2	0.15	0.22	1.36	0.005	0.015	0.82	0.52	0.013	0.15	Bal.

2. Experimental procedures

2.1. Materials and specimens

A533B3 steel plates with four sulfur content levels ranging from 0.006 wt.% (weight percent) to 0.027 wt.% were manufactured according to the specifications of ASTM A533. The materials were rolled from a thickness of 150 mm to 30 mm and solution treated at 900 °C for 1.5 h, then quenched and tempered at 670 °C for 1.5 h. A508 class 3 (hereafter abbreviated as A508) forged steels with sulfur content levels of 0.005 wt.% and 0.015 wt.% were manufactured by the specifications of ASTM A508. Their chemical compositions and mechanical properties are given in Tables 1–4, respectively.

Table 4
Mechanical properties of A508 cl. 3 steels.

Designation	Temperature (°C)	Ultimate tensile strength (MPa)	Yield strength (MPa)	Total elongation (%)	Uniform elongation (%)
F1	25	703	588	23.7	8.8
	300	670	525	16.2	7.5
F2	25	728	590	22.2	10.2
	300	684	559	18.2	9.3

Table 5
Test conditions of high-temperature water environments.

Test parameters	Air-saturated (with filtered air)	Deoxygenated (with nitrogen)	HWC
Pressure, MPa	10	10	10
Temperature, °C	300	300	300
Conductivity (inlet), μS cm^{-1}	0.8	0.08	0.065
Conductivity (outlet), μS cm^{-1}	1.2	0.16	0.072
Hydrogen (inlet),	N.A.	N.A.	48 ppb
Hydrogen (outlet),	N.A.	N.A.	39 ppb
Oxygen (inlet)	7.4 ppm	1–10 ppb	1–10 ppb
Oxygen (outlet)	6.7 ppm	1–10 ppb	1–10 ppb
ECP (SHE)	0.2 volt	−0.55 volt	−0.6 volt
pH (inlet)	5.95	6.88	6.58
pH (outlet)	6.17	6.74	6.76
Autoclave exchange rate	1 time/h	1 time/h	1 time/h

2.2. Fatigue crack growth rate tests

According to the ASTM E 647 specifications, compact-tension type (CT) specimens with a thickness of 12.5 mm and a width of 50 mm were machined. Before fatigue testing, all specimens were

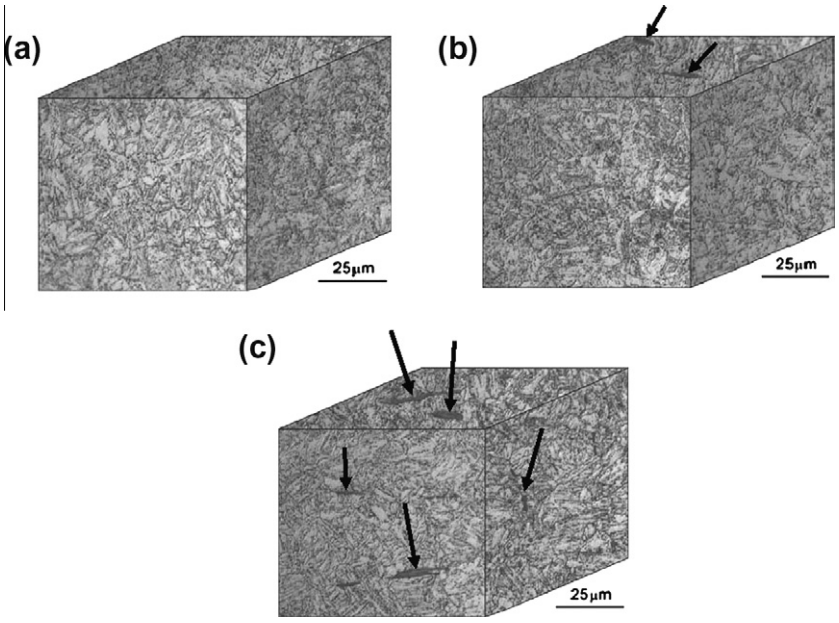

Fig. 1. Metallographs of A533B3 steels with different sulfur contents, (a) 0.008 wt.%, (b) 0.016 wt.%, (c) 0.027 wt.%. (The arrows indicate the sulfides.)

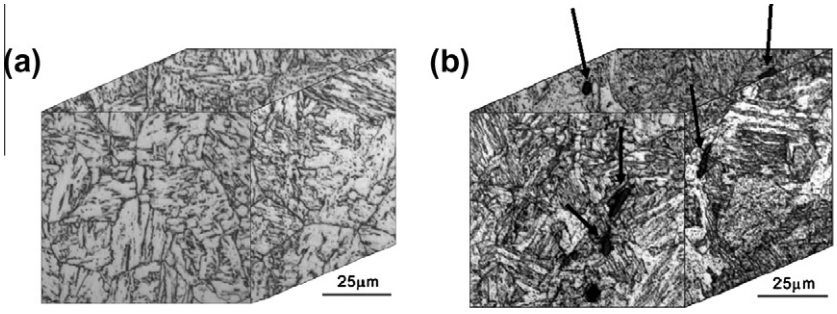

Fig. 2. Metallographs of A508 cl. 3 steels with different sulfur contents, (a) 0.005 wt.%, (b) 0.015 wt.%. (The arrows indicate the sulfides.)

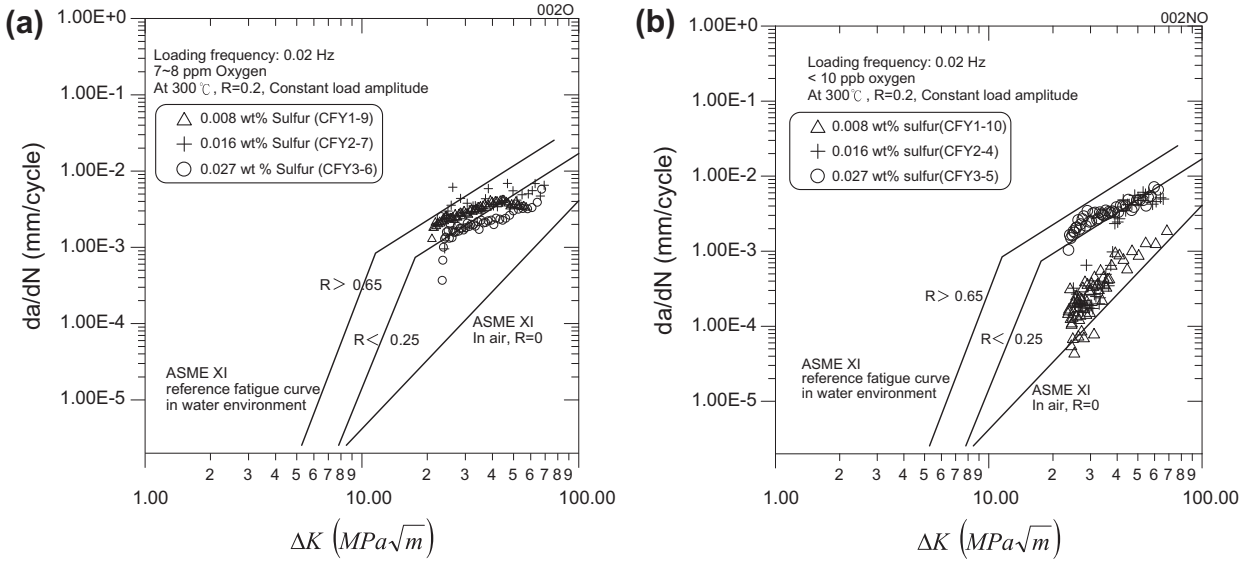

Fig. 3. Sulfur content effects on the corrosion fatigue crack growth rates of A533B3 steels with different oxygen contents in water at a loading frequency of 0.02 Hz (a) 7–8 ppm oxygen and (b) <10 ppb oxygen.

lightly polished with emery paper to #600. The specimens were pre-cracked by cyclic loading with decreasing ΔK (stress intensity factor range), at a load ratio ($R, P_{min}/P_{max}$) of 0.1, till a pre-cracked length of 3 mm and ΔK of 10 MPa $\sqrt{m}$ were reached. In order to have valid test results, the specimen was designed to be predominantly elastic for the applied ΔK values less than 50 MPa $\sqrt{m}$ as per the size requirements of the ASTM E647. The corrosion fatigue tests were conducted on a closed-loop, servo-electric machine with a water circulation loop under constant load amplitude control with a sinusoidal wave form and at the frequencies of 0.02 and 0.001 Hz, respectively. The constant load amplitude was set at an R ratio ($Load_{min}/Load_{max}$) of 0.2 by an inner load cell control, which deducted the friction force between the pulling rod and the sealing material. The external load cell measurements including the friction force were also monitored for a comparison with the ones taken by the inner load cell. The electrochemical corrosion potential (ECP) was measured with Ag/AgCl/0.1 M KCl reference electrode. The conditions of the water environment are summarized in Table 5. The crack length was measured by an alternative current potential drop (ACPD) technique. The final fatigue crack length measurement was further calibrated against the average value of five measurements taken along the crack front on the fracture surface by a microscope at a magnification of 20 according to ASTM E 647.

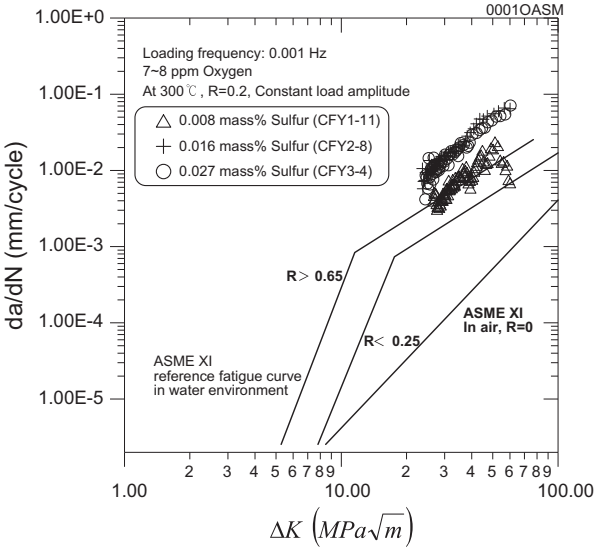

Fig. 4. Sulfur content effects on the corrosion fatigue crack growth rates of A533B3 steels in an oxygen saturated water environment at a loading frequency of 0.001 Hz.

2.3. Metallographic and fractographic examinations

To reveal the MnS morphology and carbide/nitride precipitate distribution of the low alloy steels, the as-received specimens were polished following a standard metallographic practice, then etched in a 5 vol.% Nital solution (5 vol.% nitric acid and 95 vol.% ethanol) for about 20 s and examined with optical microscopy. After corro-

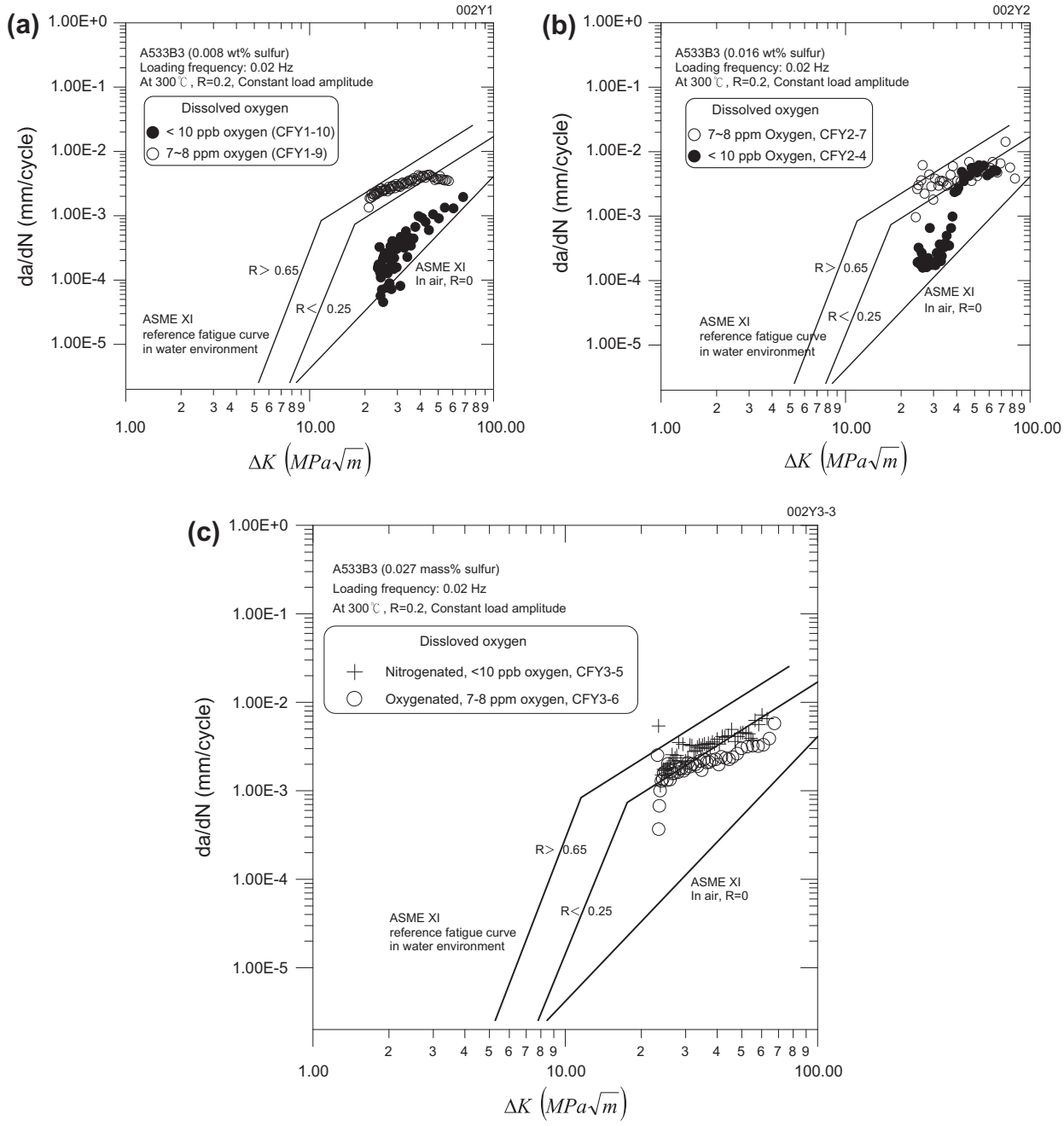

Fig. 5. A comparison of fatigue crack growth rates for A533B3 steels tested in high temperature deoxygenated and air-saturated water environments, (a) steel sulfur content 0.008 wt.%, (b) steel sulfur content 0.016 wt.%, and (c) steel sulfur content 0.027 wt.%.

sion fatigue tests, the oxide layers on the fracture surfaces were descaled with an electrolyte [16] of 2 g hexamethylene tetramine in 1000 cm^3 of 1 N HCl and further investigated with scanning electron microscopy.

3. Results and discussion

3.1. Metallographic examination

The metallographs of A533B3 and A508 steels with different sulfur contents are shown in Figs. 1 and 2, respectively. The sulfide laths identified by energy dispersive spectroscopy (EDS) were observed to be oriented in the rolling direction for A533B3 steels but A508 steels showed relatively shorter sulfides. Little or no sulfides were observed for both steels with the lowest sulfur contents. Tempered martensite was prevalent in both of the steels.

3.2. Effects of sulfur content on fatigue crack growth rate of low alloy steels

The fatigue crack growth rates of A533B3 steels with three sulfur content levels in water environments at 300 °C are shown in Fig. 3. In the air-saturated water environment, Fig. 3a, there is no significant difference between the fatigue crack growth rates for the steels with different sulfur contents at a loading frequency of 0.02 Hz. But in the deoxygenated water environment, the lower corrosion fatigue crack growth rate was observed for the steels with lower sulfur contents. For the steel with 0.016 wt.% sulfur,

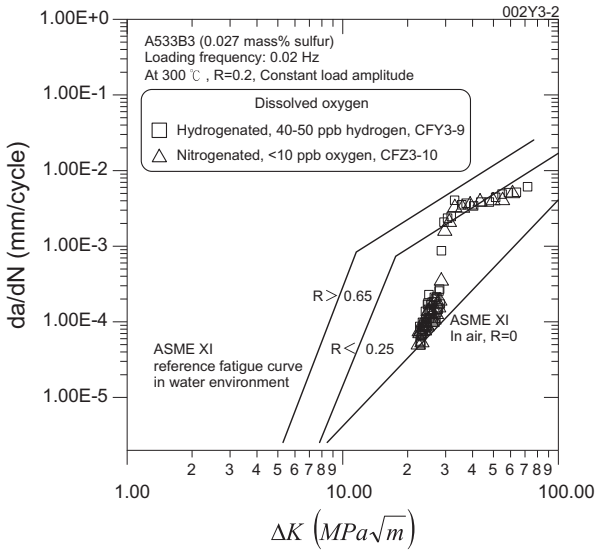

Fig. 6. A comparison of fatigue crack growth rates for A533B3 steels tested in high-temperature water environments deoxygenated by nitrogen and hydrogen, respectively.

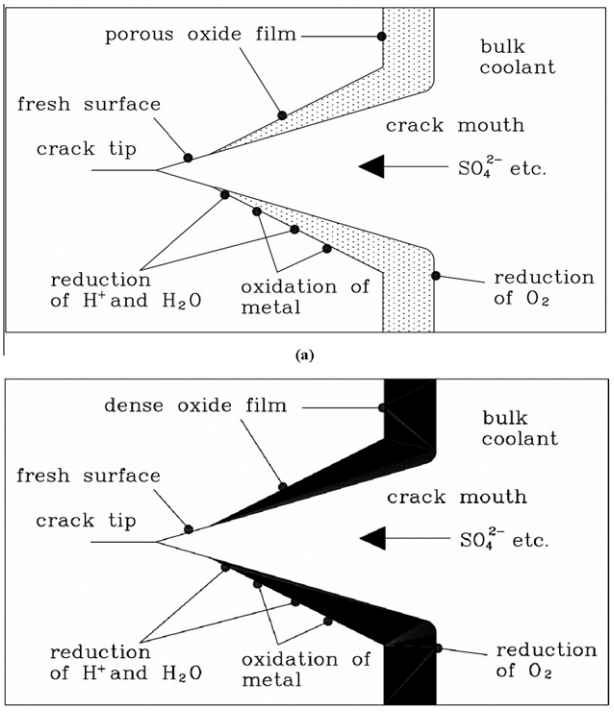

Fig. 8. A schematic illustration of different oxide films in BWR coolant environment with (a) porous oxide film formed in oxygenated water environments and (b) dense oxide film formed in deoxygenated water environment.

the corrosion fatigue crack growth rate increased significantly when the stress intensity factor range was larger than 38 MPa $\sqrt{m}$, as shown in Fig. 3b. Fig. 4 presents the results of A533B3 steel tested in an air-saturated water environment at a loading frequency of 0.001 Hz. The data outside the bounds of the ASME XI wet curves are not conservative. It was noted that the fatigue crack growth rates were almost the same for the steels of medium (0.016 wt.% sulfur) and high sulfur content (0.027 wt.% sulfur), but that those with low sulfur content showed the lowest crack growth rate. From the above results, it can be concluded that the high sulfur in low alloy steels or the high dissolved oxygen in the water coolant or their synergistic effects would degrade the corrosion fatigue resistance of low alloy steels. Therefore, it is essential to secure the integrity of pressure vessel by reducing the steel sulfur content during the steel manufacturing and by decreasing oxygen content in the reactor coolant, for instance, by HWC.

3.3. Water chemistry effects on fatigue crack growth rate

Fig. 5 makes a comparison of fatigue crack growth rates for A533B3 steels with three sulfur levels tested in deoxygenated and air-saturated water environments. It is clear that an increase in oxygen level accelerates crack growth in the steel specimens with sulfur contents up to 0.016 wt.%. For the steel with 0.027 wt.% sulfur, the opposite is true. Their corrosion fatigue crack growth rates are faster in the water environment with near zero dissolved oxygen concentration than with 7–8 ppm dissolved oxygen concentration, as shown in Fig. 5c. Fig. 6 shows a comparison of fatigue crack growth rates for high-sulfur steels tested in the high-temperature water environments deoxygenated by nitrogen and hydrogen, respectively. The fatigue crack growth rate is in good agreement with each other. Both curves show a surged crack growth rate phenomenon, similar to Fig. 5b. In Fig. 5b, for the steel specimens with 0.016 wt.% sulfur content, the fatigue crack growth rate in deoxygenated water environment surged to the same levels as those tested in saturated water environment when the concentration of sulfate ion reached a critical concentration in the crack tip. A surge of the fatigue crack growth rate occurred, when the applied $\triangle K$ reached a value of $\sim$35 MPa $\sqrt{m}$. Correspondingly, a pseudo boundary was identified on the fracture surface of the specimen, as shown in Fig. 7a. The boundary was further examined by SEM at higher magnifications to consist of a band of microcracks, which is a unique feature not observed in other regions, as shown in Figs. 7b and c. There were some inclusions imbedded in the microcracks. The inclusions containing sulfides were identified by EDS. The surged fatigue crack growth rate and a pseudo boundary were also observed with the 0.027 wt.% sulfur specimens

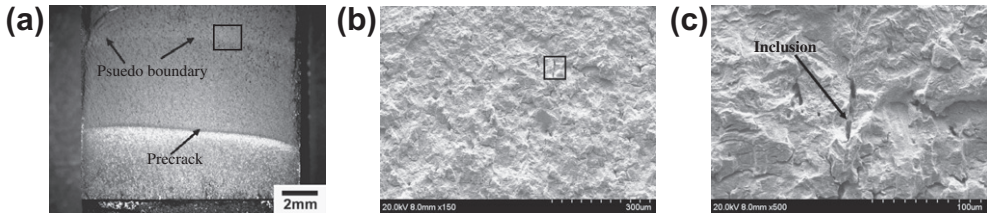

Fig. 7. A pseudo boundary observed on the fracture surface of the steel specimen with sulfur content 0.016 wt.% tested at a loading frequency of 0.02 Hz in deoxygenated water environment, (a) fractographic feature by optical stereography, (b) a band of microcracks boxed up in (a) examined by SEM, (c) microcracks boxed up in (b) at a higher magnification.

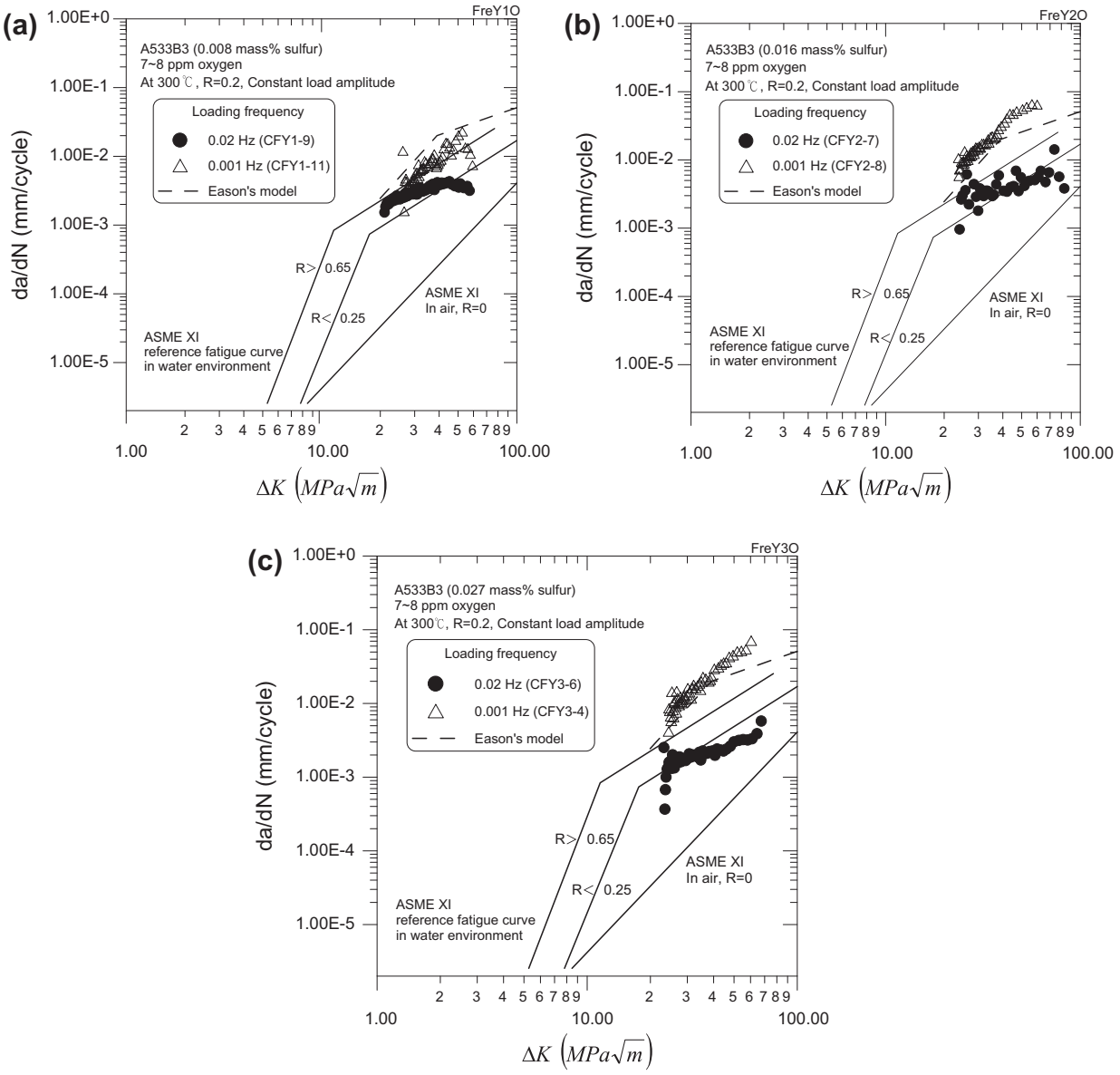

Fig. 9. Frequency effects on corrosion fatigue crack growth rates for A533B3 steels tested in high-temperature, air-saturated water environments: (a) steel sulfur content 0.008 wt.%, (b) steel sulfur content 0.016 wt.%, and (c) steel sulfur content 0.027 wt.%.

in the deoxygenated water environment, as indicated in Fig. 6. The probabilities of finding a surged fatigue crack growth rate were strongly related to the specimen sulfur levels. The greater the sulfur level, the greater the probability to find a surged growth rate. It implies the sulfides dissolved in the coolant environment around the crack tip may speed up the crack growth rate when sulfur ion reached a critical quantity. A previous study [24] showed that the dense oxide film, Fe_3O_4, was formed when low alloy steel specimens were tested in the deoxygenated water environments at 300 °C. The corrosion products in a 10 MPa water environment with saturated air at the test temperatures 300 °C were identified to be a porous mixture of Hematite (α-Fe_2O_3) and Maghemite (γ-Fe_2O_3). The porous oxide layer allows the coolant water access to the fresh metal beneath it and provides less protection than the dense one does. As a result, there was a relatively larger proportion of fresh metal on the specimens with the porous oxide layers than those with dense ones, as illustrated in Fig. 8. A hypothesis is proposed to elucidate the observation under the assumptions that sulfate ions have higher affinity to fresh metal than to the oxide layer and that the quantities of sulfate dissolved from specimens in air saturated and deoxygenated water environments are comparable. The sulfate ion in the coolant will transport to the fresh surface around the crack tip and the fresh metal beneath the porous oxide layer. In relative terms, there was less fresh metal surface of the specimen exposed to the deoxygenated water coolant than to the air-saturated one. The concentration of sulfate ion in the coolant in front of the crack tip of the specimens with dense oxide layer would be relatively larger than that with porous oxide layer. The attack of sulfate ion on the crack tip of the specimens tested in deoxygenated water environment would be more aggressive than those tested in air-saturated water environment when sulfate ions reached a critical concentration. The sulfur dissolved in the high-temperature water environment from the high-sulfur steels was sufficient to acidify the crack tip chemistry. Therefore, the deoxygenated water environment showed little or no beneficial effect for the high-sulfur steels. To mitigate the environmentally-assisted

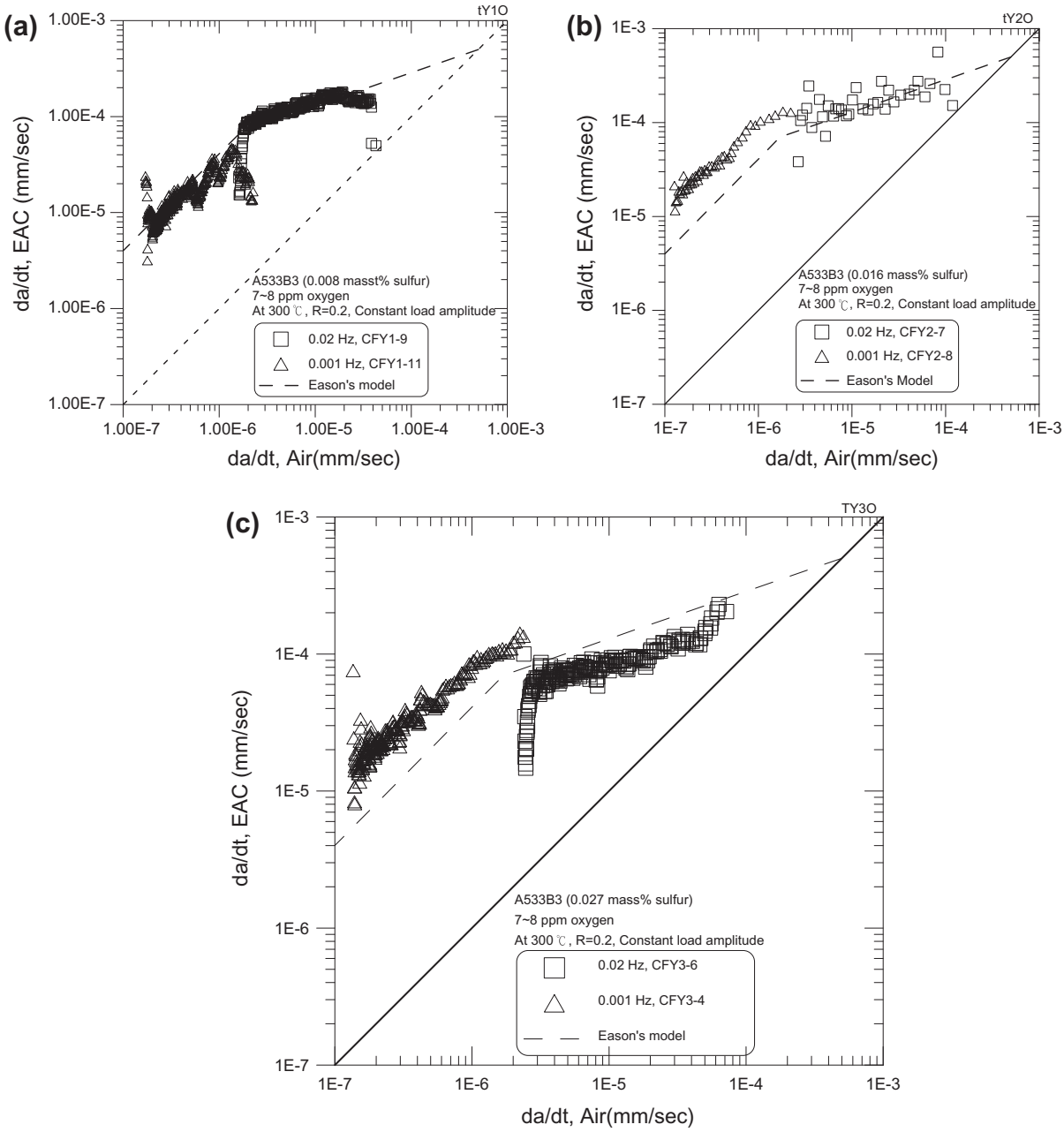

Fig. 10. Environmental effects on time-based crack growth rates for A533B3 steels tested in high-temperature, air-saturated water environments: (a) steel sulfur content 0.008 wt.%, (b) steel sulfur content 0.016 wt.%, and (c) steel sulfur content 0.027 wt.%.

cracking of low alloy steels, the factor of sulfate ion in the coolant should be taken into account.

3.4. Frequency effects on fatigue crack growth rate

Fig. 9 illustrates the frequency effects on the fatigue crack growth rate of A533 steels in the air-saturated water environment. The lower the frequency, the higher the fatigue crack growth rate was observed for all the three steel specimens with different sulfur levels. It means that the corrosion fatigue resistance of A533 steels was significantly affected by the loading frequency in the air-saturated water environment. In the GE-model [23], the corrosion fatigue (CF) crack growth through anodic dissolution is controlled by the crack-tip strain rate and the sulfur anion activity/pH in the crack tip electrolyte that govern the oxide film rupture and the dissolution/repassivation behavior after the film rupture event. From Fig. 9, the data points not bounded by the Eason's model [25] were attributed to the factors of the low frequency and higher sulfur content as well as high dissolved oxygen in the water coolant. The crack growth rates are replotted in a time basis, instead of cycle, against their counterparts in air, Fig. 10, to exemplify the environmental effect. The crack growth rates in air are derived from Eason's model,

$$da/dt = (7.87 \times 10^{-8}/\mathrm{Tr}) * [\Delta K/(2.88 - R)]^{3.07},$$

where da/dt is in mm s^{-1}, Tr is the period of rising load in seconds and $\triangle K$ is in MPa $\sqrt{m}$. The crack growth rate data for the steel with a sulfur level of 0.008 wt.% were bounded within the Eason's model.

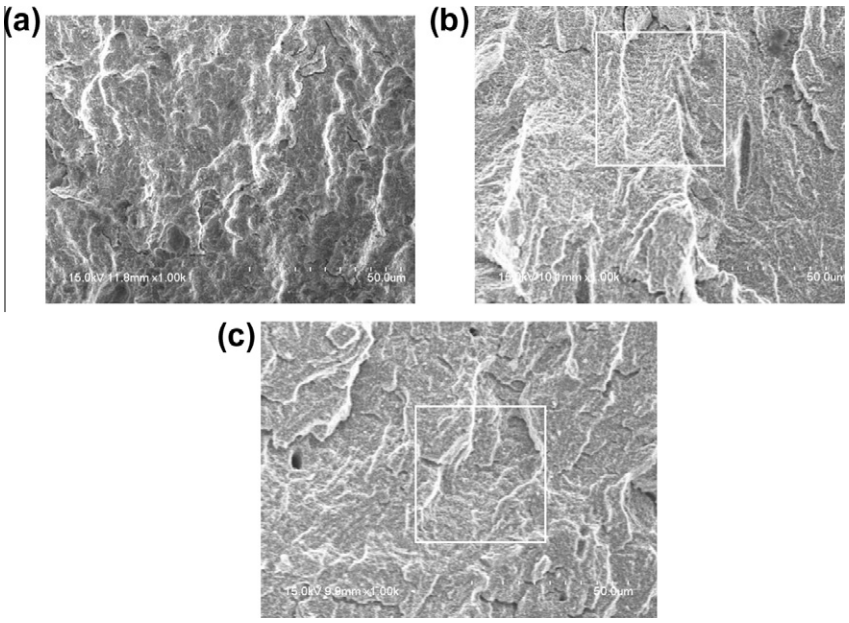

Fig. 11. SEM fractographs for A533B3 steel with sulfur content 0.016 wt.% tested in high-temperature water environments (a) 0.001 Hz, air-saturated (b) 0.02 Hz, air-saturated, (c) 0.001 Hz, deoxygenated.

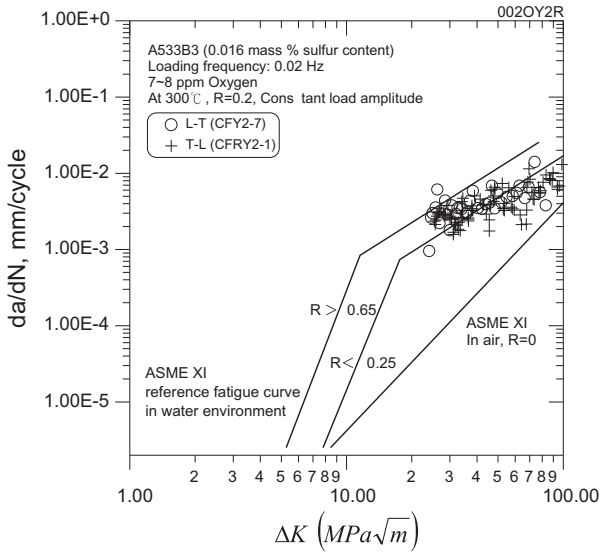

Fig. 12. Orientation on the fatigue crack growth rate of A533 steel with sulfur content 0.016 wt.% under a loading frequency of 0.02 Hz.

The loading frequency of 0.001 Hz along with high sulfur content steels (higher than 0.016 wt.%) led to more aggressive environmental effects. The data outside of Eason's model could be accounted for by the synergistic effect of high dissolved oxygen coolant, high sulfur content in steels, and low loading frequency. In Eason's model, the BWR dissolved oxygen level is below 0.4 ppm.

Distinct fracture features were revealed by SEM for the fatigue specimens tested in the high-temperature water environments at different frequencies. The fracture features were apparently related to the oxidation behavior. For the tests at a loading frequency of 0.001 Hz in the air-saturated water environment, the specimen did not reveal any fatigue striation pattern, as shown in Fig. 11a. The striations could have been corroded for a long stay in an air-saturated water environment. In the same air-saturated water environment but at a loading frequency of 0.02 Hz, the striations remained clear, illustrated in Fig. 11b. In the same way, the striations were also manifested in the deoxygenated water environment at a loading frequency of 0.001 Hz, as shown in Fig. 11c.

3.5. Effects of orientation on fatigue crack growth rate

The sulfides in A533B3 steels were oriented in the rolling direction. Previous results showed that inclusions had a deleterious effect on the smooth fatigue steel specimens [2,3]. SEM fractographs of the fatigued specimens indicated that the fatigue crack initiated at inclusion sites. From the previous study [26,27], the fatigue crack growth rate shows no dependence on the sulfur contents of A533B3 steels in air, but it is related to the specimen orientation. For the specimens with 0.016 wt.% and 0.027 wt.% sulfur tested in air at room temperature and 300 °C, the fatigue crack growth rates were faster with the crack propagation direction parallel to the rolling direction than those with the crack direction perpendicular to the specimen orientation. But in the high-temperature water environment, the corrosion fatigue crack growth rates were comparable for both orientations at the loading frequencies of 0.02 Hz, as shown in Fig. 12. That could be accounted for by the theory that corrosion fatigue crack growth rates were related to the exposure of fresh sulfide [28]. The percentage of sulfides per unit area measured by quantitative metallography was 0.012% and 0.010% for *T–L* and *L–T* orientations, respectively. So they showed the comparable crack growth rates for the steel specimens in both orientations. That means environment played a more important role than material orientation in terms of the corrosion fatigue crack growth rate.

3.6. Manufacturing processes on corrosion fatigue crack growth rate

Fig. 13 compares the corrosion fatigue crack growth rates of A533 and A508 steels. The results for the two steel specimens with ~0.015 wt.% sulfur tested at both loading frequencies of 0.001 Hz

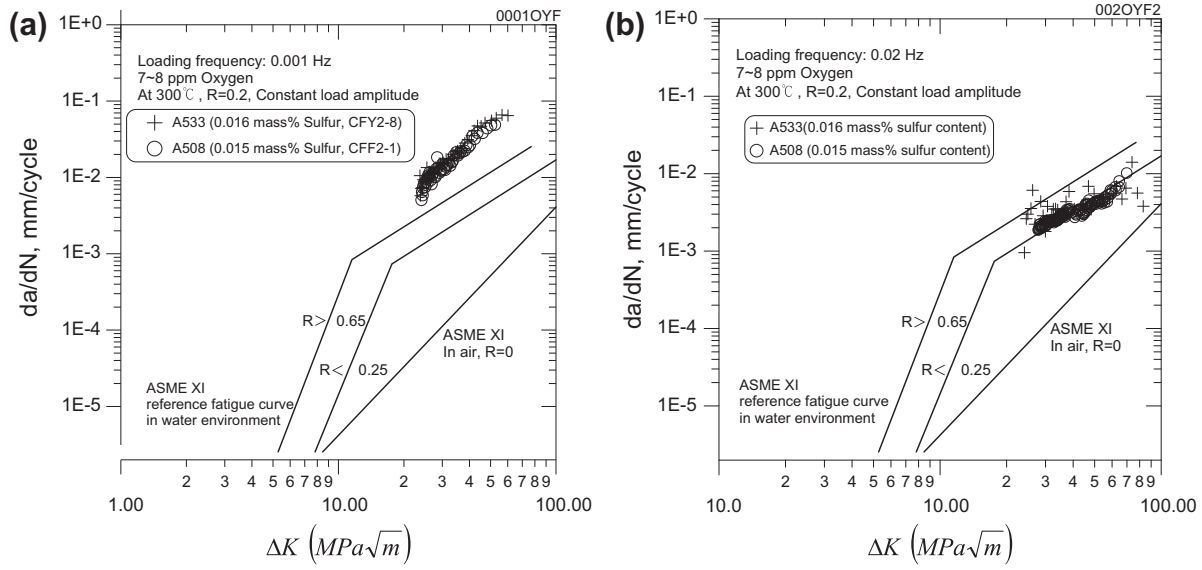

Fig. 13. A comparison of corrosion fatigue crack growth rates for A533 and A508 steels with the medium sulfur content levels under different loading frequencies, (a) 0.001 Hz, (b) 0.02 Hz.

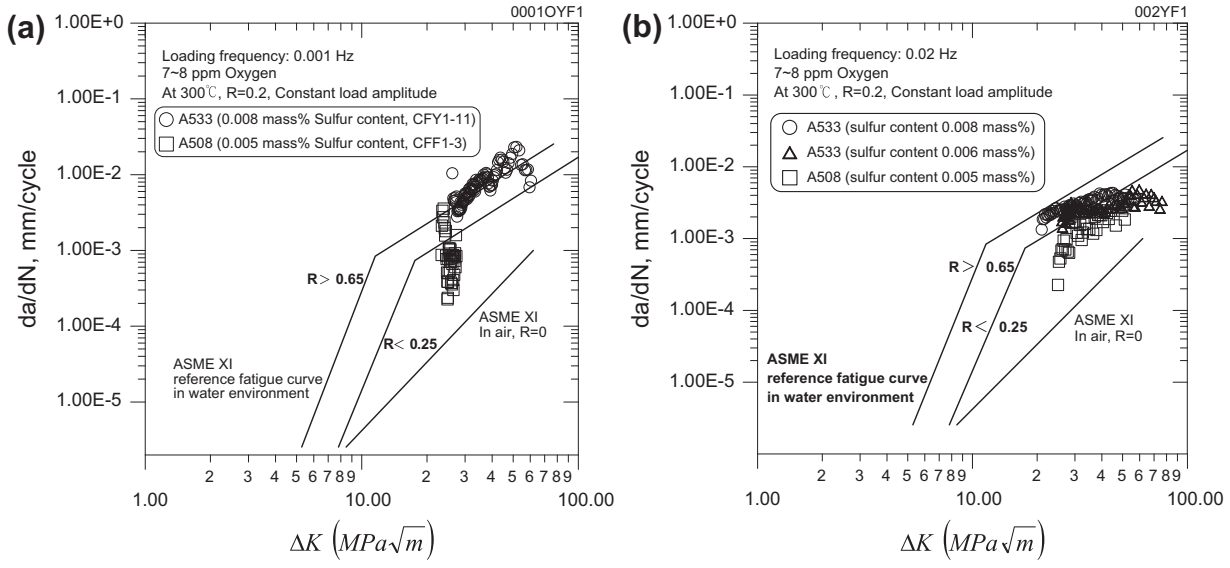

Fig. 14. A comparison of corrosion fatigue crack growth rate for A533 and A508 steels with low sulfur content levels, (a) 0.001 Hz, and (b) 0.02 Hz.

and 0.02 Hz are in a good agreement, as indicated in Figs. 13a and b, because their sulfur content levels are comparable.

A508 steel shows lower corrosion fatigue crack growth rates relative to A533 steels because A508 has a relatively lower sulfur content, even though the difference is quite small, as shown in Fig. 14. The difference of corrosion fatigue crack growth rates between A508 steel with 0.005 wt.% sulfur and A533 steel with 0.008 wt.% and 0.006 wt.% sulfur is apparent from the fatigue crack length against cycles curve, as shown in Fig. 15. So from the perspective of corrosion fatigue resistance, the sulfur content, not manufacturing process, is a concern. Atkinson [28] reported that A533B cl. 1 steel with 0.006 wt.% sulfur showed a lower fatigue crack growth rate than those with a sulfur content level 0.015 wt.%. Van Der Sluys [29,30] and Eason [25] also demonstrated little or no environmental effect on the fatigue crack growth rate of SA533 steels when their sulfur content was decreased to 0.004 wt.% and 0.005 wt.%, respectively. In this study, the steel specimens with low sulfur contents 0.005 wt.%, 0.006 wt.% and 0.008 wt.% were prepared and tested in the coolant environment. The results show that the 0.005 wt.% sulfur content could be a critical level, below that, no environmental assisted cracking was observed.

4. Conclusions

(1) Corrosion fatigue crack growth rates of A533B3 and A508 steels were significantly affected by the steel sulfur content, loading frequency and oxygen content in the high-temperature water environment. The data points outside the bound of Eason's model could be attributed to the low frequency, higher sulfur content and high dissolved oxygen water coolant.

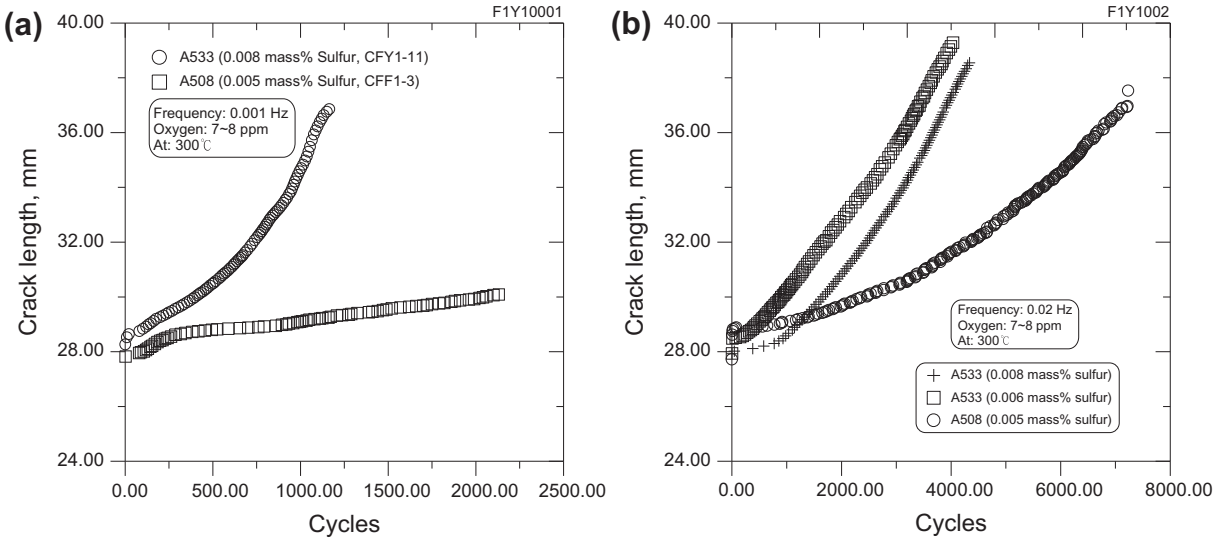

Fig. 15. Sulfur content effect on the corrosion fatigue crack rate for A533 and A508 steels with low sulfur contents, (a) 0.001 Hz, (b) 0.02 Hz.

(2) The sulfur dissolved in the water environment from the higher-sulfur steels was sufficiently concentrated to acidify the crack tip chemistry even in the HWC water. Therefore, nitrogenated or HWC water did not show any beneficiary effect on the high-sulfur steels.
(3) The corrosion fatigue crack growth rates for the steels with different orientations were comparable, which could be related to the exposure of fresh sulfide. The percentage of sulfides per unit area was measured to be equivalent for the steel specimens of both orientations.
(4) In the range of the studied parameters, the corrosion fatigue crack growth rates decreased remarkably when the steel sulfur content was decreased to a critical level of 0.005 wt.%.

Acknowledgments

The authors would like to acknowledge the financial support from Taiwan Power Company and the Institute of Nuclear Energy Research, Taiwan.

References

[1] V.N. Shah, P.E. Macdonald, Aging and Life Extension of Major Light Water Reactor Components, Elsevier Science Publishers, Amsterdam, 1993.
[2] J.Y. Huang, R.Z. Li, K.F. Chien, R.C. Kuo, P.K. Liaw, B. Yang, J.G. Huang, Fatigue behavior of SA533–B1 steels, in: R. Chona (Ed.), Fatigue and Fracture Mechanics, vol. 32, STP 1406, ASTM, Philadelphia, PA, 2001, pp. 105–121.
[3] J.Y. Huang, C.Y. Chen, K.F. Chien, R.C. Kuo, P.K. Liaw, J.G. Huang, in: Proceedings of the Julia Weertman Symposium, TMS Fall Meeting, October 31–November 4, 1999, pp. 373–384.
[4] H.P. Seifert, S. Ritter, J. Heldt, Strain induced corrosion cracking of low-alloy reactor pressure vessel steels under BWR conditions, in: F.P. Ford, G.S. Was, J.L. Nelson (Eds.), Proceedings of the 10th International Conference on Environmental Degradation of Materials in Nuclear Power System-Water Reactors, 2001.
[5] H.P. Seifert, S. Ritter, J. Hickling, Environmentally-assisted cracking of low-alloy RPV and piping steels under LWR conditions, in: G.S. Was, L. Nelson, P. King (Eds.), Proceedings of the 11th International Conference on Environmental Degradation of Materials in Nuclear Power System-Water Reactors, 2003, pp. 73–89.
[6] J.Y. Huang, M.C. Young, S.L. Jeng, J.J. Yeh, J.S. Huang, R.C. Kuo, Corrosion fatigue behavior of an Alloy 52-A508 weldment under simulated BWR coolant conditions, in: P. King, T. Allen, J. Busby (Eds.), 13th International Conference on Environmental Degradation of Materials in Nuclear Power System, Whistler, Canada, August 19–23, 2007.
[7] J.Y. Huang, J.R. Hwang, J.J. Yeh, R.C. Kuo, C.Y. Chen, Mater. Sci. Technol. 19 (2003) 1575–1584.
[8] J.Y. Huang, J.R. Hwang, J.J. Yeh, C.Y. Chen, R.C. Kuo, J.G. Huang, J. Nucl. Mater. 324 (2004) 140–151.
[9] W.A. Van Der Sluys, R.H. Emanuels, The effect of sulfur content on the crack growth rate of pressure vessel steels in LWR environments, in: J.T.A. Roberts (Eds.), Proceedings of the 2nd International Symposium on Environmental Degradation of Materials in Nuclear Power Systems-Water Reactors, Monterrey, California, September 1985, pp. 100–107.
[10] C. Amzallag, J.L. Bernard, G. Slama, Effect of loading and metallurgical parameters on the fatigue crack growth rates of pressure vessel steels in pressurized water reactor environment, in: J.T.A. Roberts (Eds.), Proceedings of the International Symposium on Environmental Degradation of Materials in Nuclear Power Systems-Water Reactors, Myrtle Beach, South Carolina, August 1983, pp. 727–745.
[11] P. Combrade, M. Foucault, G. Slama, Effect of sulfur on the fatigue crack growth rates of pressure vessel steel exposed to PWR coolant: preliminary model for prediction of the transitions between high and low crack growth rates, in: G.J. Theus, J.R. Weeks (Eds.), Proceedings of the Third International Conference on Environmental Degradation of Materials in Nuclear Power System-Water Reactors, 1987, pp. 269–276.
[12] W.A. Van Der Sluys, W.H. Cullen, Fatigue crack growth of pressure vessel materials in light-water-reactor environments, in: R. Rungta, J.D. Gilman, W.H. Bamford (Eds.), Performance and Evaluation of Light Water Reactor Pressure Vessels, PVP-119, ASME, San Diego, CA, 1987, pp. 63–71.
[13] T.P. O'Donnell, W.J. O'Donnell, Cyclic rate-dependent fatigue life in reactor water, in: S. Yukawa (Ed.), Performance and Evaluation of Light Water Reactor Pressure Vessels, PVP-306, ASME, Honolulu Hawaii, 1995, pp. 59–69.
[14] E.D. Eason, E.E. Nelson, Analysis of fatigue crack growth rate data for A508 and A533 steels in LWR environments, EPRI TR-102793, Project 2006-20 Final Report, August 1993.
[15] A. Roth, H. Hänninen, G. Brümmer, Wachter, U. Ilg, M. Widern, H. Hoffmann, Investigation of dynamic strain aging effects of low alloy steels and their possible relevance for environmentally assisted cracking in oxygenated high-temperature water, in: G.S. Was, L. Nelson, P. King (Eds.), Proceedings of the 11th International Conference on Environmental Degradation of Materials in Nuclear Power System-Water Reactors, 2003, pp. 317–329.
[16] O.K. Chopra, W.J. Shack, Effects of LWR Coolant Environments on Fatigue Design Curves of Carbon and Low-Alloy Steels, NUREG/CR-6583, ANL-97/18, US Nuclear Regulation Commission, 1998.
[17] J.D. Atkinson, J.E. Forrest, The role of MnS inclusions in the development of environmentally assisted cracking of nuclear reactor pressure vessel steels, in: W.H. Cullen (Ed.), Proceedings of the Second International Atomic Energy Agency Specialist's Meeting on Subcritical Crack Growth, vol. 2, NUREG/CP-0067, US Nuclear Regulation Commission, Sendai, Japan, 1986, pp. 153–178.
[18] T. Shoji, K. Komai, S. Abe, H. Nakajima, Mechanistic understanding of environmentally assisted cracking of RPV steels in LWR primary coolants, in: W.H. Cullen (Ed.), Proceedings of the Second International Atomic Energy Agency Specialist's Meeting on Subcritical Crack Growth, NUREG/CP-0067, vol. 2, US Nuclear Regulation Commission, Sendai, Japan, 1986, pp. 99–117.
[19] D.R. Tice, Int. J. Press. Vess. Piping 24 (1986) 139–173.
[20] K.E. Stahlkopf, J.D. Gilman, T.U. Marstan, in: R. Rungta, J.D. Gilman, W.H. Bamford (Eds.), Performance and Evaluation of Light Water Reactor Pressure Vessels, PVP-119, ASME, San Diego, CA, 1987, pp. 1–7.
[21] W. Oldfield et al., Nuclear Plant Irradiated Steel Handbook, EPRI-NP-4797, September 1986.
[22] S. Ritter, H.P. Seifert, J. Nucl. Mater. 360 (2007) 170–176.

[23] F.P. Ford, D.E. Taylor, P.L. Andresen, Corrosion-Assisted Cracking of Stainless and Low-Alloy Steels in LWR Environments, EPRI NP-5064M, 1987.
[24] J.J. Yeh, J.Y. Huang, R.C. Kuo, Mater. Chem. Phys. 104 (2007) 125–132.
[25] E.D. Eason, E.E. Nelson, J.D. Gilman, Nucl. Eng. Des. 184 (1998) 89–111.
[26] J.Y. Huang, J.J. Yeh, R.C. Kuo, J.R. Hwang, Mater. Sci. Technol. 22 (2006) 944–954.
[27] J.Y. Huang, J.J. Yeh, R.C. Kuo, S.L. Jeng, M.C. Young, Int. J. Press. Vess. Piping 85 (2008) 772–781.
[28] J.D. Atkinson, J.E. Forrest, Corros. Sci. 25 (8/9) (1985) 607–631.
[29] W.A. Van Der Sluys, R.H. Emanuelson, Nucl. Eng. Des. 119 (1990) 379–388.
[30] W.A. Van Der Sluys, R.H. Emanuelson, Environmental acceleration of fatigue crack growth in reactor pressure vessel materials and environments, Environmentally Assisted Cracking: Science and Engineering, ASTM STP 1049, 1990. pp. 117–135.